DOI: 10.1002/vms3.1105

ORIGINAL ARTICLE

WILEY

Adipose-derived mesenchymal stem cells secrete extracellular vesicles: A potential cell-free therapy for canine renal ischaemia-reperfusion injury

Haifeng Liu[1] | Liyuan Huang[1] | Fuhao Chen[2] | Zhijun Zhong[1] | Xiaoping Ma[1] | Ziyao Zhou[1] | Suizhong Cao[1] | Liuhong Shen[1] | Guangneng Peng[1]

[1]Department of Veterinary Surgery, College of Veterinary Medicine, Sichuan Agricultural University, Chengdu, China

[2]Chongqing Fengdu Agricultural Science and Technology Development Group Co. Ltd, Chongqing, China

Correspondence
Peng Guangneng, Department of Veterinary Surgery, College of Veterinary Medicine, Sichuan Agricultural University, Chengdu 611130, China.
Email: Pgn.sicau@163.com

Funding information
National Natural Science Foundation of China, Grant/Award Number: 32002353; Natural Science Foundation of Sichuan Province, Grant/Award Number: 2022NSFSC1680

Abstract

Background: Adipose-derived mesenchymal stem cells (ADMSCs) and their extracellular vesicles (EVs) are a promising source of therapies for ischaemia-reperfusion (IR) because of their potent anti-inflammatory and immunomodulatory properties.

Objectives: The aims of this study were to explore the therapeutic efficacy and potential mechanism of ADMSC-EVs in canine renal IR injury.

Methods: Mesenchymal stem cells (MSCs) and EVs were isolated and characterised for surface markers. A canine IR model administered with ADMSC-EVs was used to evaluate therapeutic effects on inflammation, oxidative stress, mitochondrial damage and apoptosis.

Results: CD105, CD90 and beta integrin ITGB were positively expressed in MSCs, while CD63, CD9 and intramembrane marker TSG101 were positively expressed in EVs. Compared with the IR model group, there was less mitochondrial damage and reduction in quantity of mitochondria in the EV treatment group. Renal IR injury led to severe histopathological lesions and significant increases in biomarkers of renal function, inflammation and apoptosis, which were attenuated by the administration of ADMSC-EVs.

Conclusions: Secretion of EVs by ADMSCs exhibited therapeutic potential in renal IR injury and may lead to a cell-free therapy for canine renal IR injury. These findings revealed that canine ADMSC-EVs potently attenuate renal IR injury-induced renal dysfunction, inflammation and apoptosis, possibly by reducing mitochondrial damage.

KEYWORDS
apoptosis, extracellular vesicles, ischaemia-reperfusion, mesenchymal stem cells, mitochondrial damage

1 | INTRODUCTION

Over the past decade, stem cells have shown potential in regenerative medicine therapies for multiple diseases. Mesenchymal stem cells (MSCs) have emerged as a promising cell-based therapy for acute kidney injury (AKI) induced by renal ischaemia-reperfusion (IR) (Huang et al., 2022). The mechanism of MSC therapy for IR injury may involve macrophage polarisation, and nuclear factor-κB and transforming growth factor (TGF) signal pathway activation (Huang et al., 2022; Zhang et al., 2022).

Recent studies have shown that MSCs do not exert their effects through differentiation (Enam et al., 2020). Instead, MSCs are quickly eliminated by monocytes and macrophages (de Witte et al., 2018; Galleu et al., 2017). Another mechanism whereby short-lived MSCs could mediate prolonged disease-modulated effects is through the release of subcellular particles comprising lipid-bilayer-enclosed extracellular vesicles (EVs) that contain a 'cargo' of bioactive molecules and participate in cell–cell communication. In particular, the small diameter size of EVs (30–120 nm) compared to that of intact MSCs (30 μm) may allow them to avoid entrapment in the lungs, and become rapidly systemically distributed and internalised by immune and epithelial cells within the kidneys (Fazekas & Griffin, 2020).

Renal IR is the most common type of induction of clinical renal disease, including renal failure and nephritis, in both humans and animals. Usually, renal IR is inevitable in routine circumstances or surgery. A pilot study showed that renal lesions occurred immediately after renal IR and reached a maximum at 30 h post-operation (Liu et al., 2019). Accompanied by oxygen radical production, mitochondrial dysfunction and inflammation, IR injury to organs leads to a series of histopathological changes of enhanced adhesion molecules, and activation and infiltration of macrophages and neutral granulocytes related to the release of inflammatory cytokines (Pefanis et al., 2019).

Some therapeutic measures, such as preischaemic antioxidants, adrenoceptor agonists (e.g. dexmedetomidine), sulodexide and hydrogen-rich water, have been shown to be efficacious for preventing or attenuating the impacts of IR (Li et al., 2018; Yin et al., 2017). It has been demonstrated that the anti-inflammatory and immunomodulatory functions of MSCs imbue these cells with remarkable therapeutic potential to mitigate organ injury, probably via a paracrine effect of EV secretion (Lerman, 2021). Researchers have hypothesised that the combined application of adipose-derived MSCs (ADMSCs) and their EVs may be a satisfied therapeutic treatment for acute renal injury (Lin et al., 2016).

The objectives of this study were to isolate, culture and characterise ADMSCs and their EVs in dogs, and to evaluate the therapeutic ability of ADMSC-EVs in renal IR injury. We also explored the roles of ADMSC-EVs in recovery of renal function and anti-apoptosis, as well as the treatment efficacy of ADMSC-EV transplantation in a canine IR-AKI model.

2 | MATERIALS AND METHODS

Beagles aged 10–12 months were used in the study. The dogs were kept under circadian rhythm and had free access to food and water. Care and handling of the dogs were performed in accordance with the Guide for the Care and Use of Laboratory Animals published by the National Academy Press (National Institutes of Health Publication No. 85-23, 1996 revision).

2.1 | ADMSC isolation, characterisation and culture

Under anaesthesia, inguinal fat (about 5 g) was collected from the dogs for the MSC extraction procedure. Briefly, after digestions with type I collagenase (Beijing Suolaibao Technology Co., Ltd., Beijing, China), filtration and centrifugal sedimentation, ADMSCs were isolated from inguinal fat tissue and cultured (Bukowska et al., 2021) in complete culture medium supplemented with 10% EQ-foetal bovine serum at 37°C and 5% CO_2. Cells ($2.0–6.0 \times 10^6$/mL) were then characterised on the basis of the expression of common MSC markers (CD34, CD31, CD45, CD105, ITGB and CD90) (Huang et al., 2021), followed by flow cytometry (CytoFLEXS, DAPI, Hoechst Blue, Germany) of the third passage of ADMSCs.

2.2 | Induction of MSC differentiation

Passage 3 (P3) ADMSCs were inoculated in 6-well culture plates at a density of 4×10^3 cells/cm^2. To determine the differentiation ability of MSCs, the culture medium was removed from each well of the experimental group and replaced with 2 mL fresh osteogenic medium (HUXMA-90021, Cyagen, CHINA) or lipogenic medium (HUXMA-90031, Cyagen, CHINA) every 2 or 3 days. Adipocytes were identified by staining with oil red O after 14 days of lipogenic differentiation induction, and osteocytes were identified by staining with alizarin red after 21 days of osteogenic differentiation induction.

2.3 | EV isolation and characterisation

EVs were isolated from supernatants of ADMSCs (5×10^6) by ultracentrifugation. A concentrated solution was enriched in supernatants via sucrose density gradient centrifugation, as previously described (Jiang et al., 2018; Kholia et al., 2018). The prepared sucrose solution and concentrated solution were successively added to an ultracentrifugation tube at a ratio of 1:8, and centrifuged at 110,000 × g at 4°C for 70 min to collect the heavy water layer. An appropriate amount of phosphate-buffered saline (PBS) was added to resuspend the precipitate, which was centrifuged at 110,000 × g at 4°C for another 70 min. Collected precipitates were resuspended in 50–100 μL PBS.

EVs were characterised by expression of typical marker proteins and protein concentrations were determined by bicinchoninic acid assay (Beijing Solarbio Science & Technology Co., Ltd). Morphological structures were observed under transmission electron microscopy (TEM), and particle size distribution was analysed via Nanoparticle Tracking Analysis (NTA). Surface markers including exosomal markers (CD63, CD9, Tsg101) were analysed by western blotting.

2.4 | Animal models and therapeutic experiments

After adaptive feeding for 1 week, 20 beagles that were normal on physical examination, routine blood examination and kidney B-ultrasound screening were numbered and randomly divided into four groups: blank group (operation with left kidney exposure but without renal vessel clamping or right nephrectomy, $n = 5$); model group (operation with left renal vessel clamping and right nephrectomy, $n = 5$); control group (IR model with administration of PBS, $n = 5$) and experimental group (IR model with administration of EVs, $n = 5$). There was no significant difference in body weight between groups.

After induction with zolazepam, teletamine and propofol, all experimental dogs were maintained under anaesthesia with isoflurane inhalation. The left renal vessels were separated by a ventral midline incision and were clipped with a noninvasive haemostatic clip (5.7 cm; Shanghai Medical Instrument Co. Ltd., China) for 60 min to induce ischaemic injury; reperfusion injury was induced after the clip was released. Kidneys were monitored by a colour change to confirm blood reflow. Right nephrectomy was performed immediately after the clip was released. Physiological saline was infused into the abdominal cavity for lavage, and the incision was sutured in a routine manner.

After the clip was released, the renal cortex of the left kidney was injected with EVs (180 μg/kg) in the experimental group and with PBS in the control group. Serum samples were collected and stored at −80°C for further analysis after reperfusion for 3, 6, 12, 24 and 30 h. After 30 h of reperfusion, kidney tissue samples were collected by laparotomy.

Sterile instruments were used for all procedures. All surgical procedures were performed by the same trained surgeons in the same environment.

2.5 | Haematoxylin and eosin (HE) staining, terminal deoxynucleotidyl transferase-mediated dUTP nick end labelling (TUNEL) assay and TEM

Renal tissue was collected from the caudal pole of the left kidney, fixed in 10% buffered formalin, embedded in paraffin and sliced in 3 μm thick sections. Sections were stained with HE to evaluate histopathological change. Five images of each sample were analysed to compare changes among different time points after surgery. Ten fields were randomly selected at 200 different times, and 10 renal tubules in each field were scored for the degree of renal tubule injury using the Paller scoring standard (Paller et al., 1984).

Renal tissue was embedded in paraffin for immunofluorescence staining of TUNEL to observe the apoptosis of kidney cells. A small amount of renal cortex was fixed in electron microscope fixative at 4°C and stored away from light for TEM (H-7560, HITACHI, Japan) to observe mitochondrial structure.

2.6 | Enzyme-linked immunosorbent assay (ELISA)

ELISA kits (R&D Systems, Inc, Minneapolis, MN, USA) were used to detect serum concentrations of interleukin (IL)-1β, IL-10, IL-6, tumour necrosis factor (TNF)-α and cystatin C (Cys-C) in the previously collected samples, and the activities of superoxide dismutase (SOD) and myeloperoxidase (MPO), and the concentration of malondialdehyde (MDA) in renal tissue. The concentrations of serum creatinine (SCr) and blood urea nitrogen (BUN) in serum were determined by an automatic animal biochemical analyser (Catalyst One, IDEXX, USA).

2.7 | Statistical analysis

All data were analysed using SPSS 20.0 software (Statistical Package for Social Science, USA) for one-way analysis of variance (ANOVA) and *t*-tests. Results are expressed as mean ± standard deviation (SD) and $p < 0.05$ was used to indicate a significant difference. All charts were plotted using GraphPad Prism 7 (GraphPad Software, USA).

3 | RESULTS

3.1 | Isolation and characterisation of ADMSCs

Morphology of ADMSCs cultured successfully to P4 was observed under an inverted microscope. ADMSCs were cultured as 24 posterior adherent cells. Primary ADMSCs cultured for 2–4 days were spindle-shaped and polygonal. Cells reached 80% confluence after 4–5 days in culture. ADMSCs exhibited fusiform and typical spindle-shaped morphologies at P3 (Figure 1a and b).

ADMSCs induced with adipocytes and osteocytes exhibit lipogenic and osteogenic differentiation abilities, respectively. After 21 days of ADMSC culture in induction medium, lipid droplets had formed (Figure 1c) and calcium nodules were positive for alizarin-red staining (Figure 1d).

To identify the MSCs isolated, we detected surface markers (CD45, CD34, CD31, CD105, CD90, ITGB) from P3 cells using flow cytometry. Markers CD45, CD34 and CD31 exhibited 1.65%, 0.94% and 3.77% positivity, respectively, while CD105, CD90 and ITGB exhibited 97.8%, 98.45% and 85.32% positivity, respectively (Figure 1e).

3.2 | Isolation and characterisation of ADMSC-EVs

EVs morphology in the four groups was observed by TEM (Figure 2a). EVs exhibited the characteristic cup-shape morphology and were

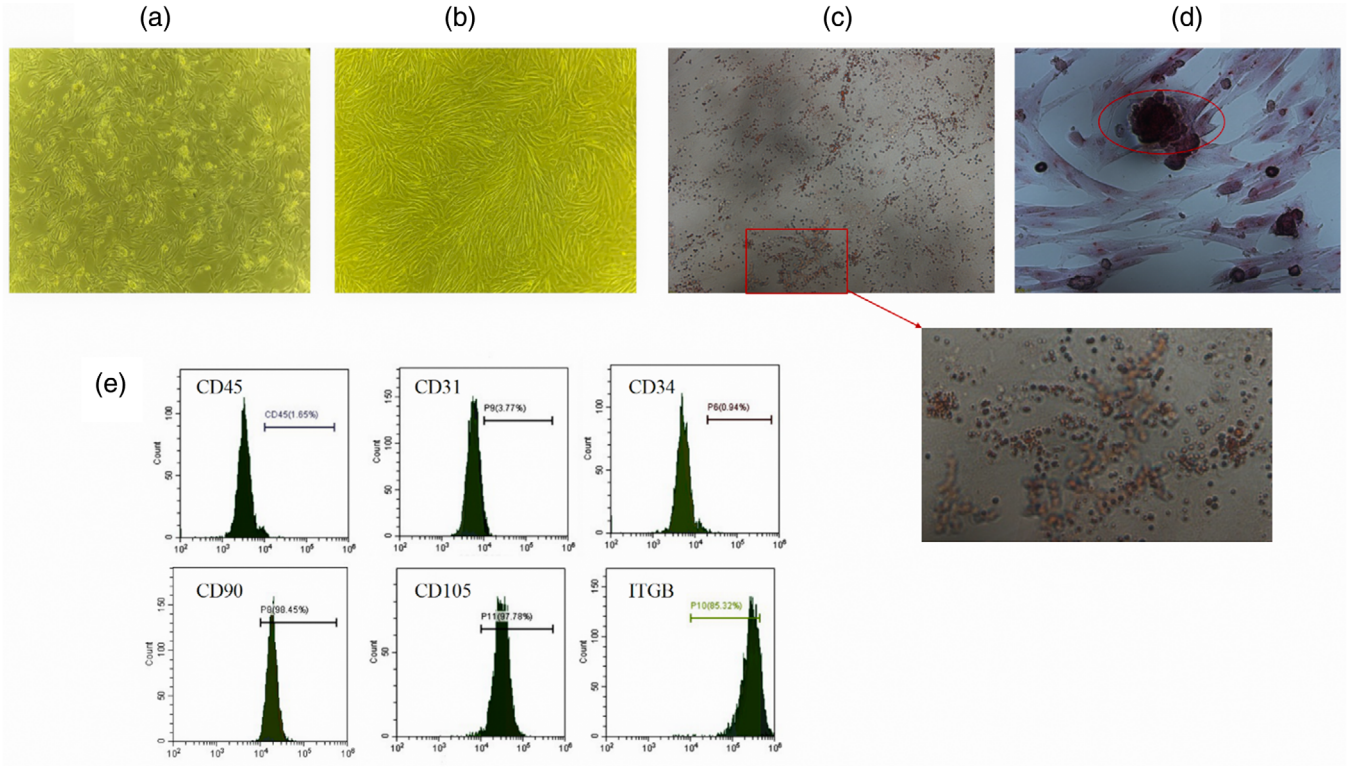

FIGURE 1 Characterisation and Differentiation of ADMSC. Morphology of canine ADMSCs P0 and P3 was observed under an inverted microscope (100×) (a, b). After 21 days of ADMSC culture in induction medium, lipogenic differentiation induction and osteogenic differentiation induction was performed successfully by staining (100×) (c, d). Markers CD45, CD34 and CD31 exhibited negatively, while CD105, CD90 and ITGB exhibited positively of ADMSC (e).

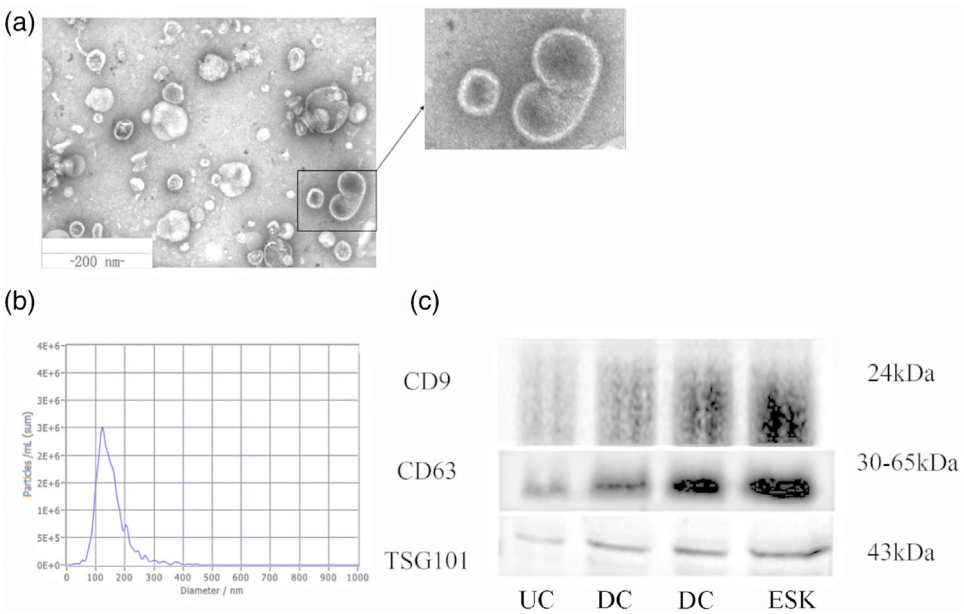

FIGURE 2 Characterisation of ADMSC-EVs. ADMSC-EVs were observed via transmission electron microscopy and characterised as cup-shape with the diameter around 30–150 nm (a). The particle size distribution of EVs samples was measured by NTA analysis (b). Western blotting against EV markers (CD9, CD63, TSG101) was performed on ADMSC-EVs (c). EVs were isolated via three methods: UC (ultracentrifugation), ESK (exosome separation Kit) and DC (density gradient centrifugation).

within the normal vesicle size range (30–150 nm in diameter). The number and average size of the EVs measured by NTA were 9.7 × 10^9/mL and 134 nm, respectively (Figure 2b). Ultramicrospectrophotometry revealed that the protein content of ADMSC-EVs was 0.36 μg/μL. Positive expression of extracellular markers (CD63, CD9) and an intramembrane marker (TSG101) were detected by western blotting (Figure 2c).

3.3 | MSC-EVs protect against renal IR injury in dogs

Renal IR resulted in markedly elevated levels of the renal function biomarkers SCr, BUN and Cys-C, as well as histopathological changes in subcellular structure, apoptosis, inflammation biomarkers TNF-α, IL-6, IL-1β and IL-10, and oxidative stress biomarkers SOD, MPO and MDA. All of these injury parameters were ameliorated by treatment with MSC-EVs.

In all groups, the concentrations of SCr and serum BUN increased post-operatively and continuously until 30 h, while that of serum Cys-C increased post-operatively but started to decrease after 24 h. Compared with the control group, following injection of ADMSC-EVs into the renal cortex, the concentrations of SCr and serum BUN dropped significantly after 24 h post-operatively, while serum Cys-C dropped significantly after 12 h post-operatively (Figure 3a).

The serum concentrations of TNF-α, IL-6, IL-1β and IL-10 increased post-operatively, then started to decrease after 12 h. Compared with the control group, following injection of ADMSC-EVs into the renal cortex, the serum concentrations of TNF-α and IL-6 were significantly lower after 3 h post-operatively, while the serum concentration of IL-10 was significantly lower after 6 h post-operatively (Figure 3b).

Histopathology showed that severe lesions emerged in renal IR injury, including tubular dilation, epithelial cell swelling, mild granular degeneration, nuclear pyknosis, cellular cast and infiltration of inflammatory cells in the renal interstitium. Administration of ADMSC-EVs in the experimental group relieved the tubular dilation, epithelial cell swelling, mild granular degeneration, cellular cast, and inflammatory cell infiltration in the renal interstitium (Figure 4a). Paller scoring also showed that the application of ADMSC-EVs alleviated renal lesions caused by IR (Figure 4b).

The serum activities of MDA and MPO increased at 30 h post-operatively and returned to normal levels when ADMSC-EVs were administered. The serum activity of SOD decreased at 30 h post-operatively and rose to normal levels when ADMSC-EVs were administered (Figure 4c).

Regarding apoptosis, the apoptotic rate was significantly higher in the model group compared with that in the blank group, but was lower in the experimental group compared with that in the model group (Figure 4d).

We also evaluated the effect of renal IR on mitochondrial morphology (Figure 4a), which is indicative of apparent mitochondrial damage. Renal IR reduced the number of mitochondria overall and increased the number of cells containing a single mitochondrion. Reduced mitochondrial matrix particles, shortened or reduced cristae, pieces of dissolved mitochondrial matrix, and cavitated mitochondria were also observed in the model group. EVs from ADMSCs partially reversed the quantitative changes and morphological damage to the mitochondria.

4 | DISCUSSION

MSCs derived from adipose tissue, the placenta and bone marrow possess the potential to attenuate multiple diseases (Han et al., 2022). MSC therapy has been successful for the treatment of several inflammatory conditions, including osteoarthritis, spinal cord injury, inflammatory bowel disease and graft-versus-host disease (Fazekas & Griffin, 2020). It is standard procedure that MSCs should be identified by surface biomarkers and the capacity to differentiate, and that their EVs should be identified by TEM, NTA and extracellular (CD63, CD9) and intramembrane (TSG101) markers (Dominici et al., 2006; Nieuwland et al., 2020).

EVs derived from MSCs exhibit potential as cell-free therapies for organ injury, tumour suppression and regulated immune response in various animals. Riazifar et al. found that MSC-EVs created a tolerogenic immune response that could be used to treat autoimmune and central nervous system disorders, decreasing the neuroinflammation and demyelination of experimental autoimmune encephalomyelitis by inhibiting the immune capacity of mice (Riazifar et al., 2019). Furthermore, there is increasing evidence that EVs derived from ADMSCs play a positive role in attenuating or preventing AKI (Aghajani et al., 2017). In the current study, we investigated the hypothesis that ADMSC-EVs protect the kidneys against renal IR injury using dogs. Additionally, this study demonstrated that treatment with ADMSC-EVs inhibits renal cell apoptosis, mitochondrial damage and production of peroxide, structurally preserving the kidneys.

IR injury stimulates histopathological damage to the renal tissues. Severe infiltration of focal inflammatory cells was observed in the renal cortex between the degenerated tubules in rats with renal IR injury. Additionally, the corticomedullary portion showed degeneration in the tubular epithelial lining, and there was aggregation of periglomerular focal inflammatory cells at the cortex in the lumen of most of these tubules (Fawzy et al., 2021). In our study, HE staining revealed that the model group exhibited renal tubular swelling, vacuolisation, necrosis and detachment of tubular basement membranes, all of which showed improvement in the experimental group. Additionally, the degree of renal tubule injury evaluated by the Paller scoring standard (Toback, 1992) demonstrated that intervention with ADMSC-EVs effectively mitigated the damage caused by renal IR.

The urinary protein BUN and SCr are increased in renal IR injury (Ling et al., 2017). Zeid and Sayed (2020) also found that the levels of serum and urinary Cys-C also rose significantly after 1 h in their IR injury group. Cys-C concentration in the blood is a desirable functional parameter and reflects the glomerular filtration rate. Similarly, in our study, there were significant increases in BUN, SCr and Cys-C in the model group ($p < 0.01$ vs. blank group), all of which were attenuated

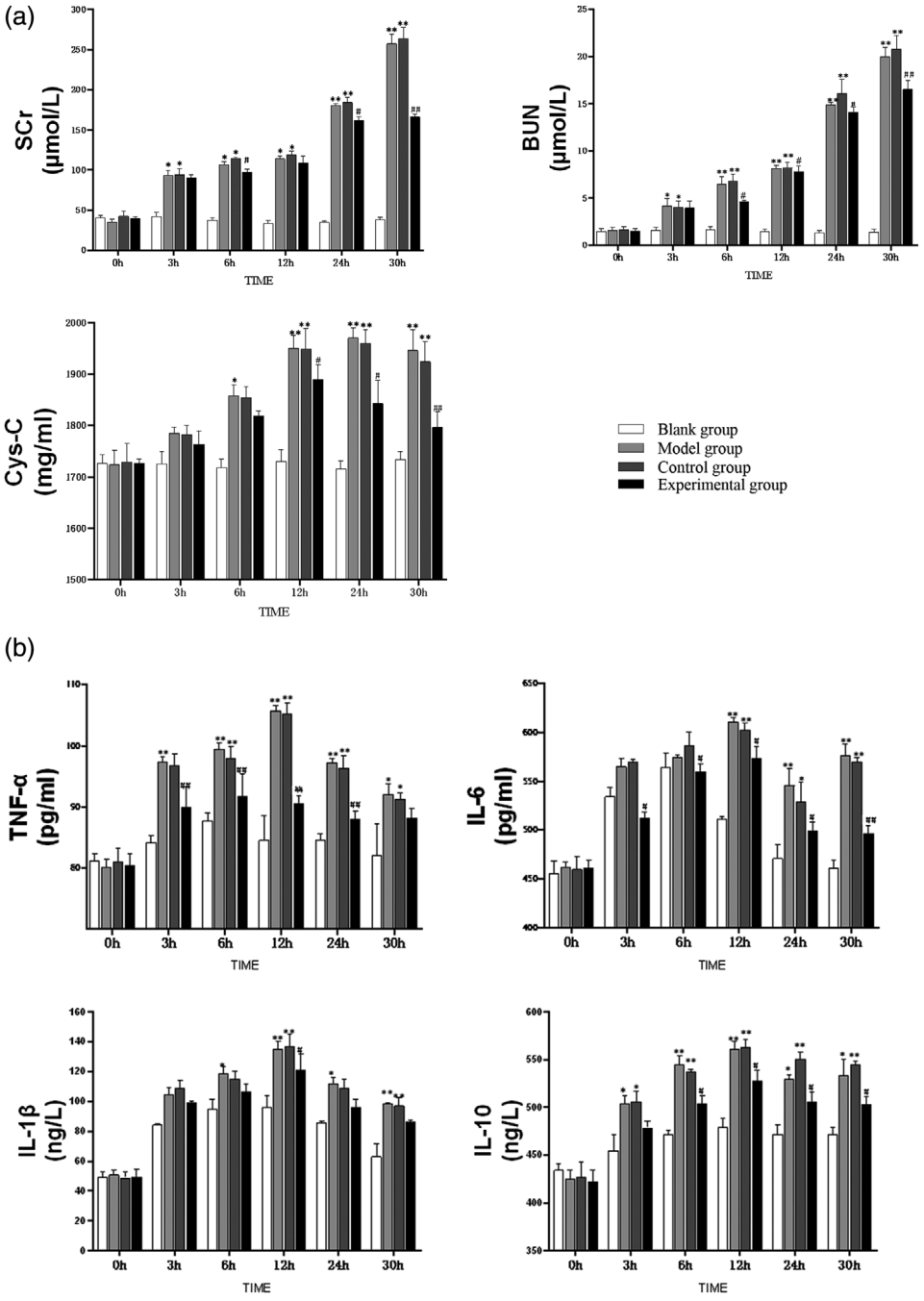

FIGURE 3 ADMSC-EVs protect renal IR from renal function and inflammatory reactions in dogs ($n = 5$). The administration of ADMSC-EVs resulted in reducing the renal function biomarkers (TNF-α, IL-6, IL-1β and IL-10) and inflammatory factors (TNF-α, IL-6, IL-1β and IL-10) to alleviate renal IR (a, b). $^{**}p < 0.01$, $^{*}p < 0.05$, vs. blank group, $\#\#p < 0.01$, $\#p < 0.05$, vs. control group at the same time point.

by administration of ADMSC-EVs. These data support the hypothesis that ADMSC-EVs attenuate renal IR injury-induced damage to renal function in vivo.

Oxidative stress, which is directly related to excessive reactive oxygen species (ROS) production in the affected tissue, plays a critical role in the pathogenesis of IR injury (Dobashi et al., 2000). Excessive production of ROS or other free radicals can lead to a switch from aerobic to anaerobic metabolic pathways, ATP depletion, cytosolic calcium overload and activation of membrane phospholipid proteolytic enzymes (Panah et al., 2018). From hypoxia to normal blood supply, IR injury leads to the production of a large number of ROS and reduced antioxidant capacity of cells (Martin et al., 2019). In this study, distinct changes in renal peroxidase activity in each group were evident at 30 h after reperfusion. After IR injury in the model group, the activity of SOD clearly dropped, and the activities of MDA and MPO rose. These conditions were alleviated in the experimental group. Several studies have shown that superoxide overproduction caused by mitochondrial injury plays a key role in IR injury (Chouchani et al., 2014; Chouchani

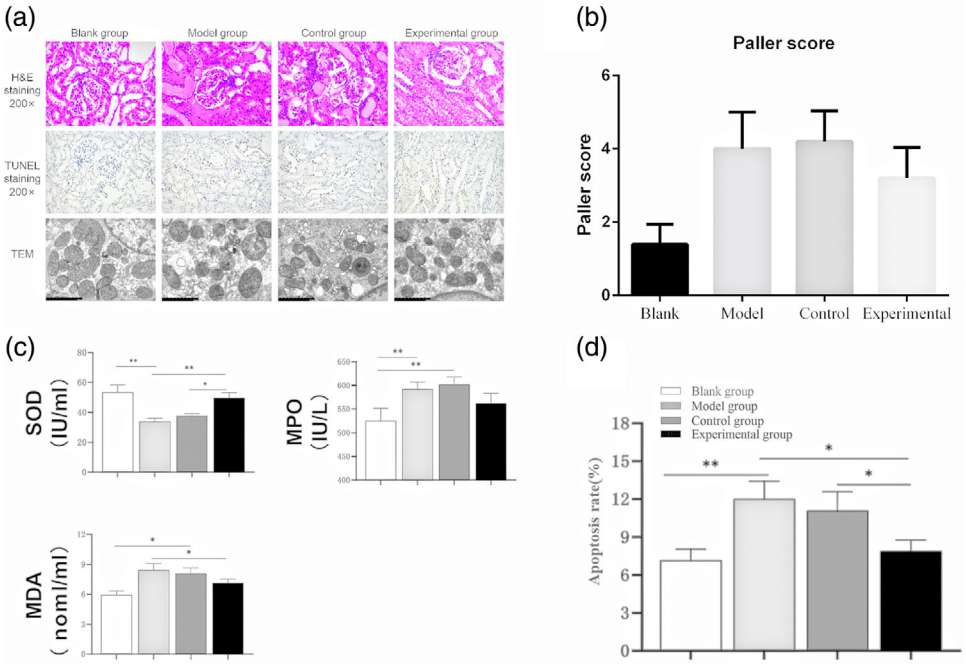

FIGURE 4 ADMSC-EVs protect renal IR from histological lesions (a, b), oxidative stress (c), mitochondrial damage (a) and cell apoptosis (a, d). ADMSC-EVs can protect against histological lesions, cell apoptosis, mitochondrial damage after 30h renal IR to alleviate renal IR (a). Renal tubule injury was evaluated by Paller scoring standard (b). The administration of ADMSC-EVs resulted in reducing renal oxidative stress (SOD, MPO, MDA) to alleviate renal IR (c). IR-induced cell apoptosis was largely alleviated after ADMSC-EVs treatment (d). Positive rate = number of positive cells/total number of cells × 100%, $^{**}p < 0.01$, $^{*}p < 0.05$.

et al., 2016). Our data support the possibility that ADMSC-EVs limit oxidative stress to maintain mitochondrial function.

Inflammatory reactions triggered by IR injury are exerted through the MAPK signalling pathway and result in increased production of inflammatory cytokines (Guo et al., 2018; Fawzy et al., 2021). Inflammatory reactions are activated immediately upon restoration of blood flow following renal ischaemia. In this study, maximum values of TNF-α, IL-6, IL-1β and IL-10 concentrations in blood were detected after 12 h of reperfusion and decreased gradually thereafter. Administration of ADMSC-EVs significantly inhibited the expression of these inflammatory cytokines at every time point.

IR injuries induce the production of ROS. The relationships between mitochondrial oxidative stress, ROS production and mitophagy are intimately interwoven (Zhang et al., 2022). Different types of cell death in kidney injury are related to mitochondrial damage. Significant damage to mitochondria may result in apoptosis, pyroptosis or ferroptosis, and recent studies showed that multiple types of cell death can be observed after IR injury (Doke & Susztak, 2022; Lu et al., 2022). Our findings also revealed that a high apoptosis rate emerged after renal IR, and that EVs derived from ADMSCs attenuated mitochondrial damage and cell apoptosis.

5 | CONCLUSIONS

The findings from this study demonstrate that canine ADMSC-derived EVs have the potential to restore immunoregulation and renal function following IR, and attenuate cell apoptosis, possibly by protecting the mitochondria. ADMSCs possess therapeutic potential in renal IR injury via secretion of EVs, which may represent a cell-free therapy for acute renal injury. Additional studies will be needed to further elucidate the mechanism of ADMSC-EV modulation of organ injury repair and immune response.

AUTHOR CONTRIBUTIONS

Conceptualisation: Haifeng Liu and Fuhao Chen. Writing – original draft: Fuhao Chen and Liyuan Huang. Writing – review & editing: Haifeng Liu and Guangneng Peng. Funding acquisition: Haifeng Liu. Supervision: Suizhong Cao and Liuhong Shen. Visualisation: Fuhao Chen and Ziyao Zhou. Methodology: Xiaoping Ma and Zhijun Zhong. All authors have read and agreed to the published version of the manuscript.

ACKNOWLEDGEMENTS

We thank Michelle Kahmeyer-Gabbe, PhD, from Liwen Bianji (Edanz) (www.liwenbianji.cn) for editing the English text of a draft of this manuscript.

CONFLICT OF INTEREST STATEMENT

The authors declare no conflict of interest.

DATA AVAILABILITY STATEMENT

The data that support the findings of this study are available from the corresponding author upon reasonable request.

ETHICS STATEMENT

This study was approved by the Sichuan Agricultural University Institutional Animal Care and Use Committee and was conducted in a manner consistent with the US National Institutes of Health 'Guide for the Care and Use of Laboratory Animals', the Animal Welfare Acts (US PL 89–544; 91–579; 94–279) and the Guide for the Care and Use of Agricultural Animals in Agricultural Research and Teaching, including appropriate methods of euthanasia (American Veterinary Medical Association Guidelines for the Euthanasia of Animals).

ORCID

Haifeng Liu https://orcid.org/0000-0002-7495-9332

PEER REVIEW

The peer review history for this article is available at https://publons.com/publon/10.1002/vms3.1105.

REFERENCES

Aghajani Nargesi, A., Lerman, L. O., & Eirin, A. (2017). Mesenchymal stem cell-derived extracellular vesicles for kidney repair: Current status and looming challenges. *Stem Cell Research & Therapy*, *8*, 273.

Bukowska, J., Szóstek-Mioduchowska, A. Z., Kopcewicz, M., Walendzik, K., Machcińska, S., & Gawrońska-Kozak, B. (2021). Adipose-derived stromal/stem cells from large animal models: From basic to applied science. *Stem Cell Reviews and Reports*, *17*, 719–738.

Chouchani, E. T., Pell, V. R., Gaude, E., Aksentijević, D., Sundier, S. Y., Robb, E. L., Logan, A., Nadtochiy, S. M., Ord, E. N., & Smith, A. C. (2014). Ischaemic accumulation of succinate controls reperfusion injury through mitochondrial ROS. *Nature*, *515*, 431–435.

Chouchani, E. T., Pell, V. R., James, A. M., Work, L. M., Saeb-Parsy, K., Frezza, C., Krieg, T., & Murphy, M. P. (2016). A unifying mechanism for mitochondrial superoxide production during ischemia-reperfusion injury. *Cell Metabolism*, *23*, 254–263.

de Witte, S. F., Luk, F., Sierra Parraga, J. M., Gargesha, M., Merino, A., Korevaar, S. S., Shankar, A. S., O'Flynn, L., Elliman, S. J., Roy, D., Betjes, M. G. H., Newsome, P. N., Baan, C. C., & Hoogduijn, M. J. (2018). Immunomodulation by therapeutic mesenchymal stromal cells (MSC) is triggered through phagocytosis of MSC by monocytic cells. *Stem Cells (Dayton, Ohio)*, *36*, 602–615.

Dobashi, K., Ghosh, B., Orak, J., Singh, I., & Singh, A. J. M. (2000). Kidney ischemia-reperfusion: Modulation of antioxidant defenses. *Molecular and Cellular Biochemistry*, *205*, 1–11.

Doke, T., & Susztak, K. (2022). The multifaceted role of kidney tubule mitochondrial dysfunction in kidney disease development. *Trends in Cell Biology*, *32*(10), 841–853.

Dominici, M., Le Blanc, K., Mueller, I., Slaper-Cortenbach, I., Marini, F., Krause, D., Deans, R., Keating, A., Prockop, D., & Horwitz, E. (2006). Minimal criteria for defining multipotent mesenchymal stromal cells. The International Society for Cellular Therapy position statement. *Cytotherapy*, *8*, 315–317.

Enam, S. F., Kader, S. R., Bodkin, N., Lyon, J. G., & Bellamkonda, R. V. (2020). Evaluation of M2-like macrophage enrichment after diffuse traumatic brain injury through transient interleukin-4 expression from engineered mesenchymal stromal cells. *Journal of Neuroinflammation*, *17*(1), 197.

Fawzy, M. A., Maher, S. A., Bakkar, S. M., El-Rehany, M. A., & Fathy, M. (2021). Pantoprazole attenuates MAPK (ERK1/2, JNK, p38)-NF-kappaB and apoptosis signaling pathways after renal ischemia/reperfusion injury in rats. *International Journal of Molecular Sciences*, *22*(19), 10669.

Fawzy, M. A., Maher, S. A., Bakkar, S. M., El-Rehany, M. A., & Fathy, M. J. (2021). Pantoprazole attenuates MAPK (ERK1/2, JNK, p38)–NF-κB and apoptosis signaling pathways after renal ischemia/reperfusion injury in rats. *International Journal of Molecular Sciences*, *22*, 10669.

Fazekas, B., & Griffin, M. D. (2020). Mesenchymal stromal cell-based therapies for acute kidney injury: Progress in the last decade. *Kidney International*, *97*, 1130–1140.

Galleu, A., Riffo-Vasquez, Y., Trento, C., Lomas, C., Dolcetti, L., Cheung, T. S., von Bonin, M., Barbieri, L., Halai, K., Ward, S., Weng, L., Chakraverty, R., Lombardi, G., Watt, F. M., Orchard, K., Marks, D. I., Apperley, J., Bornhauser, M., Walczak, H., … Dazzi, F. (2017). Apoptosis in mesenchymal stromal cells induces in vivo recipient-mediated immunomodulation. *Science Translational Medicine*, *9*(416), eaam7828.

Guo, X., Jiang, H., Chen, J., Zhang, B. F., Hu, Q., Yang, S., Yang, J., & Zhang, J. J. I. J. O. M. M. (2018). RP105 ameliorates hypoxia/reoxygenation injury in cardiac microvascular endothelial cells by suppressing TLR4/MAPKs/NF-κB signaling. *International Journal of Molecular Medicine*, *42*, 505–513.

Han, Y., Yang, J., Fang, J., Zhou, Y., Candi, E., Wang, J., Hua, D., Shao, C., & Shi, Y. (2022). The secretion profile of mesenchymal stem cells and potential applications in treating human diseases. *Signal Transduction and Targeted Therapy*, *7*, 92.

Huang, C., Meng, M., Li, S., Liu, S., Li, L., Su, Y., Gao, H., He, S., Zhao, Y., Zhang, M. J., & Biology, D. (2022). Umbilical cord mesenchymal stem cells ameliorate kidney injury in MRL/Ipr mice through the TGF-β1 pathway. *Frontiers in Cell and Developmental Biology*, *10*, 876054.

Huang, M., Li, D., Chen, J., Ji, Y., Su, T., Chen, Y., Zhang, Y., Wang, Y., Li, F., Chen, S., Dong, Y., Li, Q., Wu, L., Feng, Z., Wu, J., Zhang, L., Li, Z., Cai, G., & Chen, X. (2022). Comparison of the treatment efficacy of umbilical mesenchymal stem cell transplantation via renal subcapsular and parenchymal routes in AKI-CKD mice. *Stem Cell Research & Therapy*, *13*, 1–11.

Huang, R., Liu, L., Li, B., Qin, L., Huang, L., Yeung, K. W., & Han, Y. (2021). Nanograins on Ti-25Nb-3Mo-2Sn-3Zr alloy facilitate fabricating biological surface through dual-ion implantation to concurrently modulate the osteogenic functions of mesenchymal stem cells and kill bacteria. *Journal of Materials Science & Technology*, *73*, 31–44.

Jiang, L., Liu, X.-Q., Ma, Q., Yang, Q., Gao, L., Li, H.-D., Wang, J.-N., Wei, B., Wen, J., Li, J., Wu, Y. G., & Meng, X. M. (2018). hsa-miR-500a-3P alleviates kidney injury by targeting MLKL-mediated necroptosis in renal epithelial cells. *FASEB Journal: Official Publication of the Federation of American Societies for Experimental Biology*, *33*(3), 3523–3535. https://doi.org/10.1096/fj.201801711R

Kholia, S., Sanchez, M., Cedrino, M., Papadimitriou, E., & Camussi, G. J. (2018). Human Liver stem cell-derived extracellular vesicles prevent aristolochic acid-induced kidney fibrosis. *Frontiers in Immunology*, *9*, 1639.

Lerman, L. O. (2021). Cell-based regenerative medicine for renovascular disease. *Trends in Molecular Medicine*, *27*(9), 882–894.

Li, H., Bai, G., Ge, Y., Zhang, Q., Kong, X., Meng, W., & Wang, H. (2018). Hydrogen-rich saline protects against small-scale liver ischemia-reperfusion injury by inhibiting endoplasmic reticulum stress. *Life Sciences*, *194*, 7–14.

Lin, K. C., Yip, H. K., Shao, P. L., Wu, S. C., Chen, K. H., Chen, Y. T., Yang, C. C., Sun, C. K., Kao, G. S., Chen, S. Y., Chai, H. T., Chang, C. L., Chen, C. H., & Lee, M. S. (2016). Combination of adipose-derived mesenchymal stem cells (ADMSC) and ADMSC-derived exosomes for protecting kidney from acute ischemia-reperfusion injury. *International Journal of Cardiology*, *216*, 173–185.

Ling, Q., Yu, X., Wang, T., Wang, S. G., Ye, Z. Q., & Liu, J. H. (2017). Roles of the exogenous H2S-mediated SR-A signaling pathway in renal ischemia/reperfusion injury in regulating endoplasmic reticulum stress-induced autophagy in a rat model. *Cellular Physiology and Biochemistry: International Journal of Experimental Cellular Physiology, Biochemistry, and Pharmacology*, *41*, 2461–2474.

Liu, H. F., Meng, W. J., Kong, X. D., Bai, G., Li, H., Zhang, J. T., Fan, H.-G., & Wang, H.-B. (2019). Partial (two-thirds) nephrectomy in pigs: A comparison of three surgical approaches. *Research in Veterinary Science*, *125*, 459–464.

Lu, T., Zhang, J., Cai, J., Xiao, J., Sui, X., Yuan, X., Li, R., Li, Y., Yao, J., & Lv, G. J. B. (2022). Extracellular vesicles derived from mesenchymal stromal cells as nanotherapeutics for liver ischaemia–reperfusion injury by transferring mitochondria to modulate the formation of neutrophil extracellular traps. *Biomaterials*, *284*, 121486.

Martin, J. L., Gruszczyk, A. V., Beach, T. E., Murphy, M. P., & Saeb-Parsy, K. J. (2019). Mitochondrial mechanisms and therapeutics in ischaemia reperfusion injury. *Pediatric Nephrology (Berlin, Germany)*, *34*, 1167–1174.

Nieuwland, R., Falcon-Perez, J. M., Thery, C., & Witwer, K. W. (2020). Rigor and standardization of extracellular vesicle research: Paving the road towards robustness. *Journal of Extracellular Vesicles*, *10*, e12037.

Paller, M. S., Hoidal, J. R., & Ferris, T. F. (1984). Oxygen free radicals in ischemic acute renal failure in the rat. *Journal of Clinical Investigation*, *74*, 1156–1164.

Panah, F., Ghorbanihaghjo, A., Argani, H., Zarmehri, M. A., & Ahmad, S. N. S. J. C. (2018). Ischemic acute kidney injury and klotho in renal transplantation. *Clinical Biochemistry*, *55*, 3–8.

Pefanis, A., Ierino, F. L., Murphy, J. M., & Cowan, P. J. (2019). Regulated necrosis in kidney ischemia-reperfusion injury. *Kidney International*, *96*, 291–301.

Riazifar, M., Mohammadi, M. R., Pone, E. J., Yeri, A., Lasser, C., Segaliny, A. I., McIntyre, L. L., Shelke, G. V., Hutchins, E., Hamamoto, A., Calle, E. N., Crescitelli, R., Liao, W., Pham, V., Yin, Y., Jayaraman, J., Lakey, J. R. T., Walsh, C. M., Van Keuren-Jensen, K., … Zhao, W. (2019). Stem cell-derived exosomes as nanotherapeutics for autoimmune and neurodegenerative disorders. *ACS Nano*, *13*, 6670–6688.

Su, L., Zhang, J., Gomez, H., Kellum, J. A., & Peng, Z. (2022). Mitochondria ROS and mitophagy in acute kidney injury. *Autophagy*, *19*(2), 401–414.

Toback, F. G. (1992). Regeneration after acute tubular necrosis. *Kidney International*, *41*, 226–246.

Yin, J., Chen, W., Ma, F., Lu, Z., Wu, R., Zhang, G., Wang, N., & Wang, F. (2017). Sulodexide pretreatment attenuates renal ischemia-reperfusion injury in rats. *Oncotarget*, *8*, 9986–9995.

Zeid, A. S. S., & Sayed, S. (2020). A comparative study of the use of dexamethasone, N-acetyl cysteine, and Theophylline to ameliorate renal ischemia–reperfusion injury in experimental rat models: A biochemical and immuno-histochemical approach. *Saudi Journal of Kidney Diseases and Transplantation: An Official Publication of the Saudi Center for Organ Transplantation, Saudi Arabia*, *31*, 982.

Zhang, Y., Le, X., Zheng, S., Zhang, K., He, J., Liu, M., Tu, C., Rao, W., Du, H., Ouyang, Y., Li, C., & Wu, D. (2022). MicroRNA-146a-5p-modified human umbilical cord mesenchymal stem cells enhance protection against diabetic nephropathy in rats through facilitating M2 macrophage polarization. *Stem Cell Research & Therapy*, *13*, 1–16.

How to cite this article: Liu, H., Huang, L., Chen, F., Zhong, Z., Ma, X., Zhou, Z., Cao, S., Shen, L., & Peng, G. (2023). Adipose-derived mesenchymal stem cells secrete extracellular vesicles: A potential cell-free therapy for canine renal ischaemia-reperfusion injury. *Veterinary Medicine and Science*, *9*, 1134–1142. https://doi.org/10.1002/vms3.1105